BMC Cancer

RESEARCH

Open Access

Ethoxy-erianin phosphate inhibits angiogenesis in colorectal cancer by regulating the TMPO-AS1/miR-126-3p/PIK3R2 axis and inactivating the PI3k/AKT signaling pathway

Shaoqun Liu[1,2†], Fei Teng[1,2†], Yuxin Lu[3†], Yanqing Zhu[3], Xin Liang[3], Fanhong Wu[5,6], Jianwen Liu[3,6], Wenming Zhou[4*], Chang Su[1,2*] and Yiou Cao[1,2*]

Abstract

Colorectal cancer (CRC) is the third most common malignancy, with increasing prevalence and mortality. How the ethoxy-erianin phosphate (EBTP) mediates CRC development remains unclear. Therefore, the current study evaluated the effects of EBTP on the proliferation, migration, and angiogenesis of CRC cells using CCK-8, Wound-healing, Transwell, and Tube formation assays. RNA sequencing and molecular docking techniques helped predict that EBTP could inhibit angiogenesis by regulating PIK3R2 expression while clarifying the mechanism behind EBTP-mediated CRC angiogenesis. Subsequently, several in vitro experiments indicated that PIK3R2 overexpression significantly improved the proliferation, migration, and angiogenesis of CRC cells while knocking down PIK3R2 expression inhibited their proliferation, migration, and angiogenesis. Simultaneously, PIK3R2 expression in CRC cells gradually decreased with increased EBTP concentration and action duration. Moreover, PIK3R2 overexpression in CRC cells could reverse the inhibitory EBTP effect in angiogenesis. Mouse experiments also depicted that EBTP inhibited CRC angiogenesis by down-regulating PIK3R2 expression. In addition, EBTP could inhibit PI3K/AKT pathway activity and indirectly control PIK3R2 expression through the lncRNA TMPO-AS1/miR-126-3p axis. Our findings highlighted that EBTP could inhibit CRC angiogenesis using the TMPO-AS1/miR-126-3p/PIK3R2/PI3k/AKT axis, providing a novel strategy for anti-angiogenic therapy in CRC.

Keywords EBTP, Colorectal cancer, Angiogenesis, PIK3R2, TMPO-AS1

†Shaoqun Liu, Fei Teng and Yuxin Lu are co-first authors.

*Correspondence:
Wenming Zhou
23099145@qq.com
Chang Su
suchang_jx@126.com
Yiou Cao
yioucao_doctor@126.com
Full list of author information is available at the end of the article

Introduction

Colorectal cancer (CRC) is the third most common malignancy worldwide because of risk factors like lack of exercise, low-fiber diet, smoking, and obesity, with its mortality rate ranking second [1, 2]. Current advances in chemotherapy, targeted therapy, immunotherapy, and other treatments have improved the overall survival of CRC patients. However, the mortality rate of these patients remains high. Tumor metastasis, a major cause of death in CRC patients, is a complex process involving multiple pathways and uses the ability of cancer cells to migrate, invade, and develop angiogenesis [3, 4]. As tumor angiogenesis plays a crucial role in tumor metastasis, anti-angiogenic therapy is a significant breakthrough in treating metastatic CRC. During the last decade, new targeted agents have emerged for treating malignancies, primarily anti-angiogenic agents [5]. Therefore, developing new agents for treating CRC and exploring the specific mechanisms controlling angiogenesis is crucial.

Erianin is a natural product isolated from *Dendrobium ferruginum* and *Dendrobium bullae* and is a promising anti-cancer molecule [6]. We used the basic principles of drug design to structurally modify erianin and obtain EBTP while improving its structural instability and poor solubility (Fig. 1A) [7]. Previously, EBTP exhibited antiproliferative activity against breast cancer cells MCF-7, cervical cancer cells Hela, and lung cancer cells 2LL. Furthermore, EBTP could inhibit cell migration and disrupt the vascular system inside fertilized eggs [7]. On the other hand, combining EBTP and afatinib inhibited angiogenesis in hepatocellular carcinoma cells by regulating vascular endothelial growth factor (VEGF) and epidermal growth factor receptor (EGFR) signaling pathways [8]. However, whether EBTP could effectively mediate angiogenesis in CRC remains unclear, increasing the demand for investigating the exact mechanism.

Phosphoinositide 3-kinase (PI3K) is a heterodimer with regulatory (p85) and catalytic (p110) subunits. PI3K is classified into three classes based on its structure, with class I PI3K being the most typical [9, 10]. The PI3K pathway abnormalities are often considered a cancer hallmark [11]. Phosphatidylinositol-3-kinase regulatory subunit 2 (PIK3R2) is a ubiquitous isoform encoding the subunit p85β of class I PI3K [12]. Recent studies have depicted that aberrant PIK3R2 expression is involved in mediating the development and progression of various human cancers [13, 14]. For instance, PIK3R2 can improve glioma cell proliferation through the PI3K/AKT axis [15]. While inducing prostate cancer cell metastasis, Song observed that PIK3R2 was upregulated in prostate cancer tissues [16]. Although PIK3R2 can control the malignant process as an oncogene in various tumors, no evidence exists on the role of PIK3R2 in CRC angiogenesis.

We demonstrated through various functional experiments that EBTP could effectively inhibit the proliferation, migration, and angiogenesis within CRC cells. Additional in vivo and in vitro experiments depicted that the ability of EBTP to inhibit angiogenesis was obtained by downregulating PIK3R2 expression in CRC cells. Meanwhile, EBTP could control PIK3R2 expression through the lncRNA TMPO-AS1/miR-126-3p axis. Thus, the downstream PI3K/AKT pathway phosphorylation was inhibited, inhibiting angiogenesis in CRC. Our results provided a new strategy for the anti-angiogenic treatment of CRC.

Materials and methods

Cell culture and reagents

Human colon cancer cells HCT116 and SW480 and human umbilical vein endothelial cells HUVEC were obtained from the Chinese Academy of Sciences cell bank. HCT116 and SW480 cells were cultured in DMEM medium with 10% fetal bovine serum and HUVEC in ECM medium with 5% fetal bovine serum. All the cells were kept in an incubator containing 5% CO_2 at 37 °C.

Prof. Wu Fanhong of the Shanghai University of Applied Technology provided EBTP (CAS Registry Number: 1221157-01-2) with 98% purity. EBTP was dissolved in a phosphate-buffered saline (PBS) solution, configured as a 1 mM master mix and stored at -20 °C.

RNA sequencing

The logarithmic growth stage HCT116 cells were inoculated into a six-well culture plate. After the cells adhered to the wall, the blank control group was replaced using a fresh culture medium. In contrast, the drug-added group continued cultivating for 24 h with 4 μM EBTP. Then, the medium was discarded, washed thrice using clean PBS, 1 mL of TRIZOL was added to each well, and frozen for 5 min for lysis. The supernatant was stored in dry ice, and RNA sequencing was performed using the sequencing company.

(See figure on next page.)

Fig. 1 EBTP inhibits the proliferation, migration, and angiogenesis of colorectal cancer cells. **A** The chemical structural formula of EBTP. **B** CCK-8 assay helped detect the effect of different EBTP concentrations on the proliferation capability of CRC cells. **C** The transwell assay helped detect EBTP change in the migration potential of CRC cells. **D** EBTP effect on CRC cell migration was observed with the Wound-healing assay. **E** A Transwell experiment helped determine the EBTP effect on the cell migration ability of HUVEC. **F** The experiment of Tube formation tested the EBTP effect on HUVEC's ability to develop tubes. **G** Western blot experiments helped investigate the VEGF-A, VEGFR1, and VEGFR2 protein expression in CRC cells. All the experiments were independently repeated thrice. *$p < 0.05$; **$p < 0.01$; ***$p < 0.001$; ****$p < 0.001$

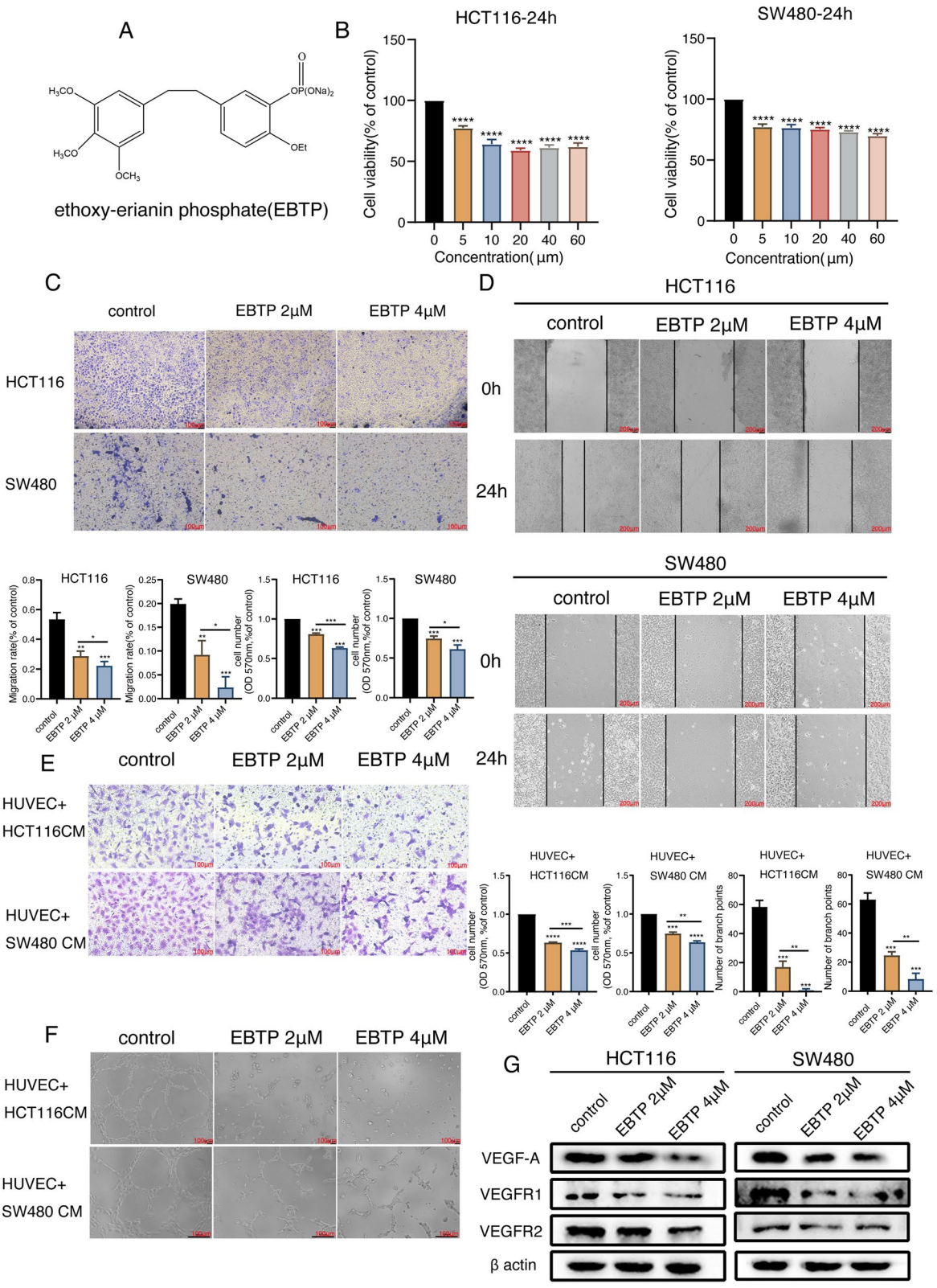

Fig. 1 (See legend on previous page.)

Cell transfection

PIK3R2-pcDNA (pcDNA3.1-WT-PIK3R2) was procured from Shanghai Joiner Bio. The shRNA sequence (5'-GAC AACAGAGAGAGATCGACAAG-3') was constructed in the pLent-U6-GFP-Puro vector to extract the PIK3R2 knockdown plasmid (Shanghai DNA Bioscience Co. Ltd. Shanghai, China). We purchased Sh-TMPO-AS1, miR-126-3p mimics, miR-126-3p inhibitor, and their respective controls from GenePharma (Shanghai, China). HCT116 and SW480 cells were transfected using a lipo8000 transfection reagent (Beyotime Biotechnology, Shanghai, China). Total RNA was extracted after 24 h of transfection, and total protein was extracted after 48 h. The transfection efficiency was tested with RT-qPCR and Western Blot.

CCK-8 assay

The viability and proliferative capacity of the CRC cells were evaluated with CCK-8 (Elabscience, Biotechnology Co., Ltd.). Briefly, 100 μL of CRC cells were inoculated in 96-well plates within the logarithmic growth phase at a density of 1×10^5/mL and were treated following the experimental groupings after 24 h. 10 μL of CCK-8 solution was added, and the absorbance was measured at 450 nm after incubating for 1 h at 37 °C.

Preparation of conditioned medium (CM)

CRC cells were inoculated in six-well plates and were processed according to the experimental groups after cell walling. The supernatants were obtained after 24 h from the EBTP-added group. Cell supernatants were collected after 48 h from CRC cells transfected using PIK3R2 OE/KD (an appropriate amount of EBTP was added to the drug-added group after transfecting for 24 h). Similarly, cell supernatants were obtained from CRC cells transfected with miR-126-3p inhibitor or sh-TMPO-AS1 after 48 h. The supernatant was centrifuged at 5000 rpm for 15 min, and the cell supernatant was kept at -20 ℃ for subsequent experiments.

Transwell assay

CRC cells treated with EBTP for 24 h or transfected with PIK3R2 OE/KD plasmid for 48 h were diluted to 2×10^5/mL cell suspension using a medium with 1% fetal bovine serum. 200 μL of cell suspension was inoculated in the upper chamber of Transwell (Corning, NY, USA). Then, 500 μL of complete medium with 10% fetal bovine serum was kept in the lower chamber. After 24 h, the cells were passed through the chambers and stained with crystal violet, and five randomly selected areas were photographed. The crystalline violet was dissolved in methanol, and the absorbance was measured at 570 nm using an enzyme marker.

Wound-healing assay

CRC cells were inoculated in a 6-well plate in the logarithmic growth phase. After the density reached 100%, the cell supernatant was discarded, and the cells were scratched using the tip of a sterile pipette (10 μL). The images were photographed and recorded under a microscope. The medium was altered to EBTP-containing or EBTP-free serum-free, and the culture was continued for 24 h before photographing the scratches.

Tube formation assay

Matrigel (Yeasen Biotechnology, Shanghai, China) was dissolved at 4 °C overnight, and the 96-well plates were pre-cooled inside a 4 °C refrigerator. Each well was placed inside an incubator for 30 min at 37 °C after adding 50 μL of matrigel to solidify. HUVECs were diluted to 2×10^5/mL with different groupings of conditioned medium. 100 μL of cell suspension was introduced to the matrigel-coated 96-well plate and incubated for 4 h. Five randomly selected fields of view were photographed under the microscope, and the number of tubes was determined with the Image J software.

Protein extraction and western blot

Total cellular proteins were retrieved using RIPA lysate (Beyotime Biotechnology, Shanghai, China). Protein quantification was performed using the Bradford method. 30 μg of protein was electrophoresed in SDS-PAGE and transferred onto PVDF membranes (250 mA, 2 h). After blocking, the membranes were incubated overnight at 4 °C with antibodies: VEGF-A (Cat. No. WL00009b, Wanlei Bio, China), VEGFR1 (Cat. No. AF6204, Affinity, China), VEGFR2 (Cat. No. AF6281, Affinity, China), PIK3R2 (Cat. No. AF2951, Affinity, China), PI3K (Cat.

(See figure on next page.)

Fig. 2 PIK3R2 promotes the proliferation, migration, and angiogenesis of HCT116 cells. **A** The molecular docking technique helped simulate EBTP binding to PIK3R2. **B** PIK3R2 expression in CRC and non-cancerous tissues in the HPA site. **C** Western Blot helped verify the transfection efficiency of PIK3R2 in HCT116 cells. **D** qRT-PCR could verify PIK3R2 overexpression and knockdown efficiency among HCT116 cells. **E** CCK-8 assay for HCT116 cell proliferation. **F** A Transwell experiment helped determine the PIK3R2 expression effect on HCT116 cell migration. **G** The Transwell assay explored the change impact on the migration ability of HUVEC in PIK3R2 expression inside HCT116 cells. **H** The Tube formation experiment explored the effect of changes on the ability of HUVEC to develop tubes in PIK3R2 expression in HCT116 cells. **I** Western Blot assay helped detect the expression of VEGF pathway-related proteins in HCT116 cells. All the experiments were independently repeated thrice. *$p<0.05$; **$p<0.01$; ***$p<0.001$

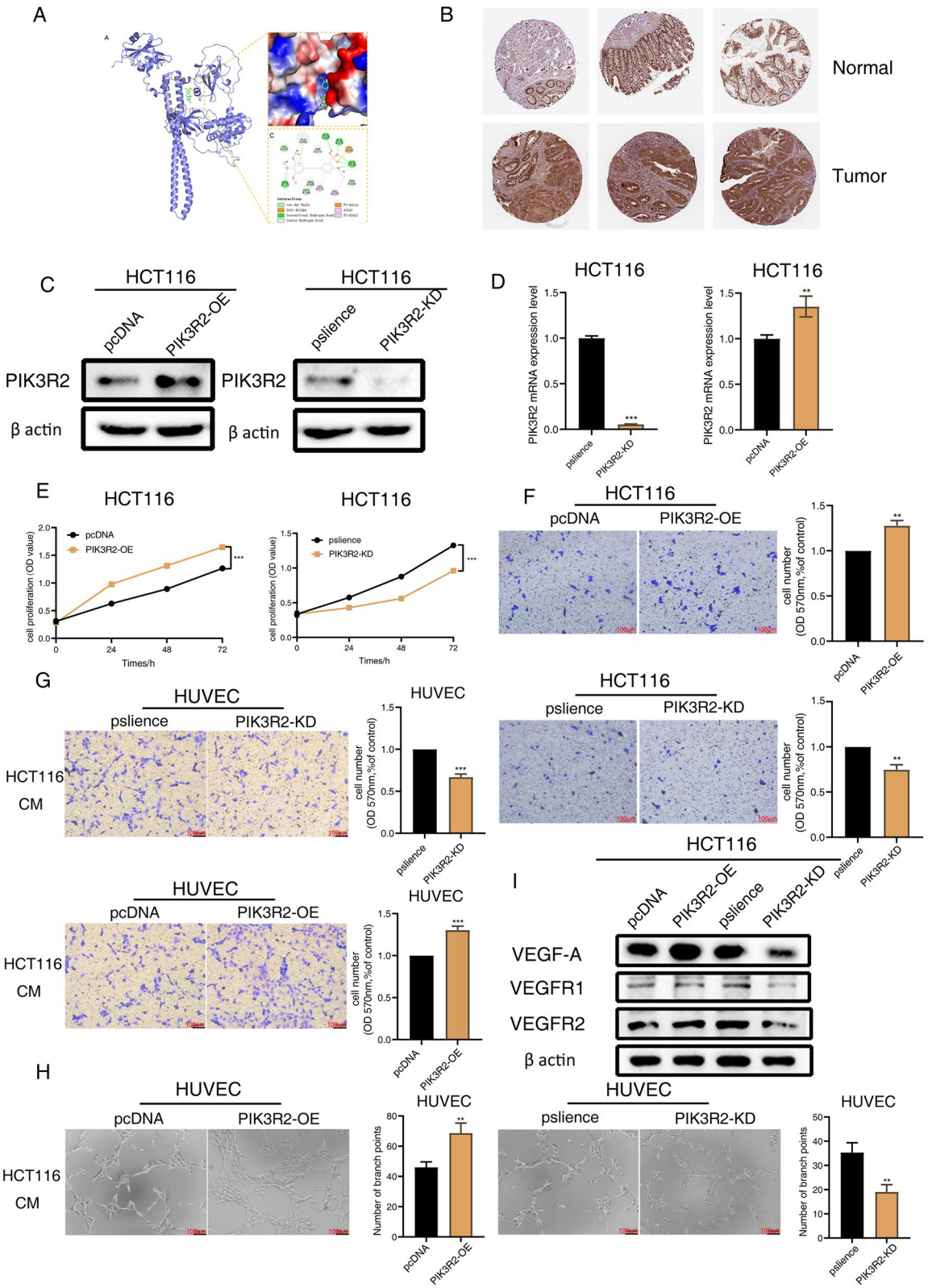

Fig. 2 (See legend on previous page.)

No. 4292, Cell Signaling, USA), P-PI3K (Cat. No. 4228, Cell Signaling, USA), AKT (Cat. No. CY5561, Abways, China), P-AKT (Cat. No. CY6569, Abways, China), and β-actin (Cat. No. AB0035, Abways, China). The membranes were rinsed and incubated using an enzyme-labeled secondary antibody (Cat. No. E-AB-1003, Elabscience, China) at room temperature the next day for 2 h. Membranes were cut horizontally. A Tanon imaging system (5200 S) helped detect protein bands after binding to ECL chemiluminescent reagents.

Molecular docking

The chemical structure of EBTP was retrieved from the PubChem database (https://pubchem.ncbi.nlm.nih.gov/). Later, Chem3D software helped import, optimize, and minimize energy using the MM2 module. The protein structure of PIK3R2 (PDB ID: AF-O00459-F1) was obtained from the UniProt database (https://www.uniprot.org/uniprotkb/O00459) and processed on the Maestro11.9 platform. The protein was treated using Schrodinger's Protein Preparation Wizard to remove the water of crystallization, add missing hydrogen atoms, and repair missing bond information and peptide segments. Finally, the protein was energy minimized and optimized in geometric structure.

The Glide module of the Schrödinger Maestro software helped process and optimize molecular docking. Protein processing used the Protein Preparation Wizard module. Receptors were pre-processed, optimized, and minimized (constrained minimization with the OPLS3e force field). Compound structures were prepared according to the default settings of the LigPrep module. For screening in the Glide module, the designed receptors were imported, and the docking sites were predicted based on the structural characteristics of the protein while setting the docking box to 20Åx20Åx20Å. Finally, Standard Precision (SP) helped perform molecular docking and screening.

RNA extraction and quantitative real-time fluorescent quantitative PCR (qRT-PCR)

Total RNA was extracted from CRC cells using TRIzol™ reagent (Sigma, USA). They were reverse transcribed into cDNA according to the manufacturer's instructions (Cat. No. 11119ES60, Yeasen Biotechnology, China). The relative expression of PIK3R2, TMPO-AS1, and miR-126-3p was analyzed using Hieff UNICON qPCR SYBR Green Master Mix (Yeasen Biotechnology, Shanghai, China). GAPDH (PIK3R2 and TMPO-AS1) and U6 (miR-126-3p) became normalization controls. TMPO-AS1, miR-126-3p, U6, and GAPDH primers are represented in Table S1.

Xenograft model

Twenty five-week-old male BALB/c nude mice were randomly divided into four groups, with five in each group. We resuspended 5×10^6 wild-type or HCT116 cells transfected with PIK3R2 overexpression plasmid in 50% matrix gel solution (V/V, saline: matrix gel = 1:1). They were injected subcutaneously into different nude mice groups. After the subcutaneous tumor volume reached 100 mm^3, the three groups were administered with gavage (EBTP, 50 mg/kg) for 21 days according to the body weight of the mice. After the administration, the animals were euthanized using CO_2 asphyxiation, and the tumors were weighed to measure the volumes. All the animal experiments were performed using IACUC-approved protocols from the East China University of Science and Technology. The animal husbandry protocols followed the Declaration of Helsinki.

Immunohistochemistry (IHC)

First, we degreased and rehydrated the tumor tissue sections. The sections were immersed inside 1 mM Tris/EDTA (pH = 9.0) antigen retrieval solution, boiled for 30 min, and cooled at room temperature. After blocking using 3% BSA for 1 h, CD31 (Cat. No. AF6191, Affinity, China) and CD34 antibodies (Cat. No. CY5196, Abways, China) were incubated overnight at 4 °C. A biotinylated secondary antibody (Biological Technology, California, USA) was introduced inside the samples for 1 h. Later, Streptavidin Peroxidase Complex (SABC, Biological Technology) was added and incubated for 30 min at 37 °C. A solution of 3,3'-diaminobenzidine tetrahydrochloride (DAB, Biological Technology) was added. The sections were dehydrated and were photographed using a bright-field microscope (Olympus).

Dual-luciferase reporter assay

A dual luciferase reporter gene assay helped examine the interaction between PIK3R2/TMPO-AS1 and miR-126-3p. The binding sites of PIK3R2 (WT PIK3R2) and

(See figure on next page.)

Fig. 3 The ability of EBTP to inhibit angiogenesis in colorectal cancer depends on PIK3R2. **A** Western Blot helped test whether EBTP can inhibit the PIK3R3 protein expression in CRC cells in a time-dependent and concentration-dependent manner. **B** The PIK3R2 mRNA expression level was tested using RT-qPCR with increased EBTP treatment time or concentration within CRC cells. **C** The Transwell assay helped determine whether CRC cells transfected using PIK3R2 overexpression plasmid could reverse the EBTP effect by suppressing HUVECs migration. **D** Exploring whether PIK3R2 could reverse the EBTP phenomenon by suppressing HUVECs formation with Tube formation experiments. **E** Western blot analysis helped investigate the transfection effect of PIK3R2 overexpression plasmid on VEGF-A, VEGFR1, and VEGFR2 expression in CRC cells. All the experiments were independently repeated thrice. *$p < 0.05$; **$p < 0.01$; ***$p < 0.001$。 #$p < 0.05$; ##$p < 0.01$; ###$p < 0.001$

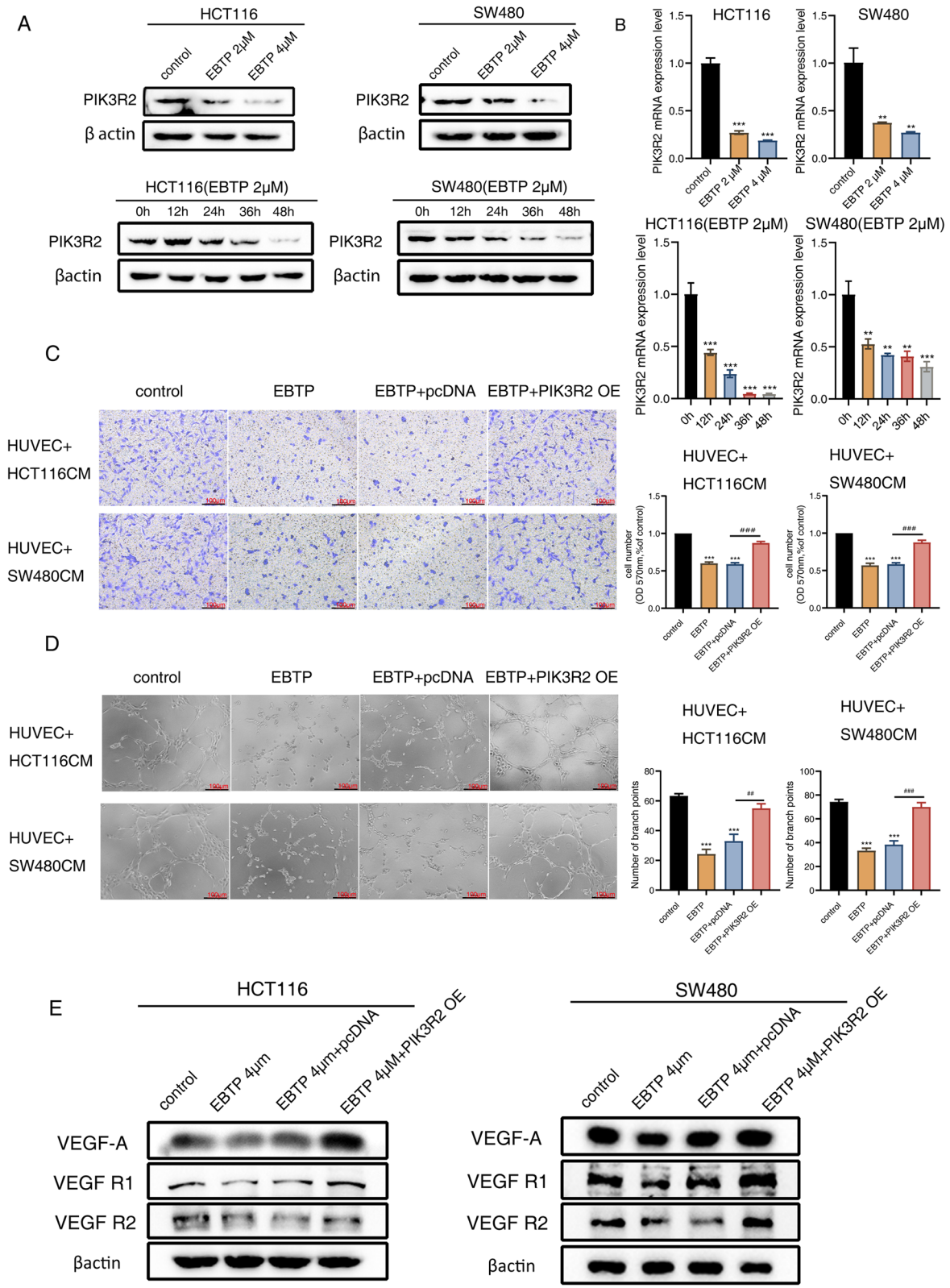

Fig. 3 (See legend on previous page.)

TMPO-AS1 (WT TMPO-AS1) were cloned to miR-126-3p, and their mutation sites (MUT PIK3R2, MUT TMPO-AS1) into the GP-miRGLO vector (GenePharma, Shanghai, China). These constructs were cotransfected with miR-126-3p mimics or NC mimics into CRC cells. The cells were assayed for luciferase activity of fireflies and sea cucumbers with a dual luciferase reporter gene assay kit after 48 h (Beyotime Biotechnology, Shanghai, China).

Bioinformatics analysis

Relevant data were retrieved from the HPA website (https://www.proteinatlas.org/) to analyze PIK3R2 expression in CRC and adjacent non-cancerous tissue sections. The GEPIA website (http://gepia.cancer-pku.cn/) helped analyze PIK3R2 expression in pan-cancer and explore this expression in CRC.

Statistical analysis

The experiments were replicated three times independently, and the data were processed using the GraphPad Prism 8.0 software. The data were uniformly processed as Mean ± Standard Deviation (SD). Significant differences were analyzed with the Student t-test, where $p < 0.05$ was considered statistically significant.

Result

EBTP inhibits the proliferation, migration, and angiogenesis of colorectal cancer cells

The effect of different concentrations of EBTP was examined on the proliferation activity of HCT116 and SW480 cells using CCK-8 to screen for appropriate EBTP concentration on CRC cells (Fig. 1B). The results indicated that EBTP significantly inhibited CRC cell proliferation. EBTP inhibited HCT116 proliferation in a concentration-dependent manner in the 0–10 μM range. In contrast, EBTP effectively inhibited SW480 proliferation in a concentration-dependent manner within the 0–5 μM range. For operational convenience, 2 μM and 4 μM were chosen to investigate the effects of EBTP on CRC cell migration and angiogenesis. According to the results of Transwell and Wound-healing assays, EBTP significantly restricted the migratory potential of HCT116 and SW480 cells. Moreover, the inhibitory ability was elevated by enhancing EBTP concentration (Fig. 1C and D). Then, we examined the EBTP effects on the migration and tube formation abilities of HUVECs using Transwell and Tube formation assays, respectively. The results are represented in Fig. 1E and F. EBTP inhibited the migration potential and tubular ability of HUVECs in a concentration-dependent manner. Our previous study observed that EBTP inhibited hepatocellular carcinoma angiogenesis through the VEGF pathway [8]. Therefore, the Western Blot assay helped investigate whether EBTP could affect the expression of VEGF pathway-related proteins in CRC (Fig. 1G). These data indicated that EBTP could effectively restrict the proliferation, migration, and angiogenesis of CRC cells.

PIK3R2 promotes the proliferation, migration, and angiogenesis of colorectal cancer cells in vitro

We sequenced RNA from HCT116 cells without or with 24 h EBTP treatment to investigate the specific mechanism of EBTP-mediated malignant biological behavior of CRC and identify the top ten differential mRNAs. PIK3R2 increased our research interest in differential mRNAs. After the literature search, several binding sites for erianin exhibited a high affinity for PI3K [17]. PIK3R2 is a common subunit of PI3K, and EBTP could bind to PIK3R2, affecting CRC angiogenesis. First, EBTP was molecularly docked with the PIK3R2 target protein. The results depicted in Fig. 2A revealed that the compound EBTP had an excellent binding effect while developing hydrogen bonds and hydrophobic interactions with the PIK3R2 protein. Therefore, EBTP could bind to PIK3R2 and inhibit malignant tumor development.

We first explored PIK3R2 expression in pan-cancer to clarify its role within the CRC process. The results suggested that PIK3R2 was highly expressed in breast, colorectal, and hepatocellular carcinomas (Figure S1A). Moreover, CRC patients showed high PIK3R2 expression compared to healthy patients (Fig. 2B and Figure S1B). We constructed PIK3R2 overexpression and PIK3R2 knockdown plasmids to investigate the role of PIK3R2 in CRC. Then, the PIK3R2 transfection effectiveness was validated in HCT116 cells using Western Blot and qRT-PCR assays (Fig. 2C and D). The high expression of PIK3R2 in HCT116 cells improved the proliferation and migration of HCT116, while the knockdown of PIK3R2 expression suppressed the proliferation and migration of HCT116 (Fig. 2E and F). Meanwhile, high PIK3R2 expression effectively improved the migratory

(See figure on next page.)

Fig. 4 EBTP inhibits the growth and angiogenesis of colorectal cancer in vivo. **A** A schematic diagram of the nude mouse xenograft model. **B** A representative image of a subcutaneous solid tumor inside nude mice. **C** The volume statistics of solid tumors in nude mice of each group. **D** The weight statistics of solid tumors in nude mice from each group. **E** Immunohistochemical detection of CD31 and CD34 expression within solid tumor tissues from each group. All the experiments were independently repeated thrice. *$p < 0.05$; **$p < 0.01$; ***$p < 0.001$。 #$p < 0.05$; ##$p < 0.01$; ###$p < 0.001$

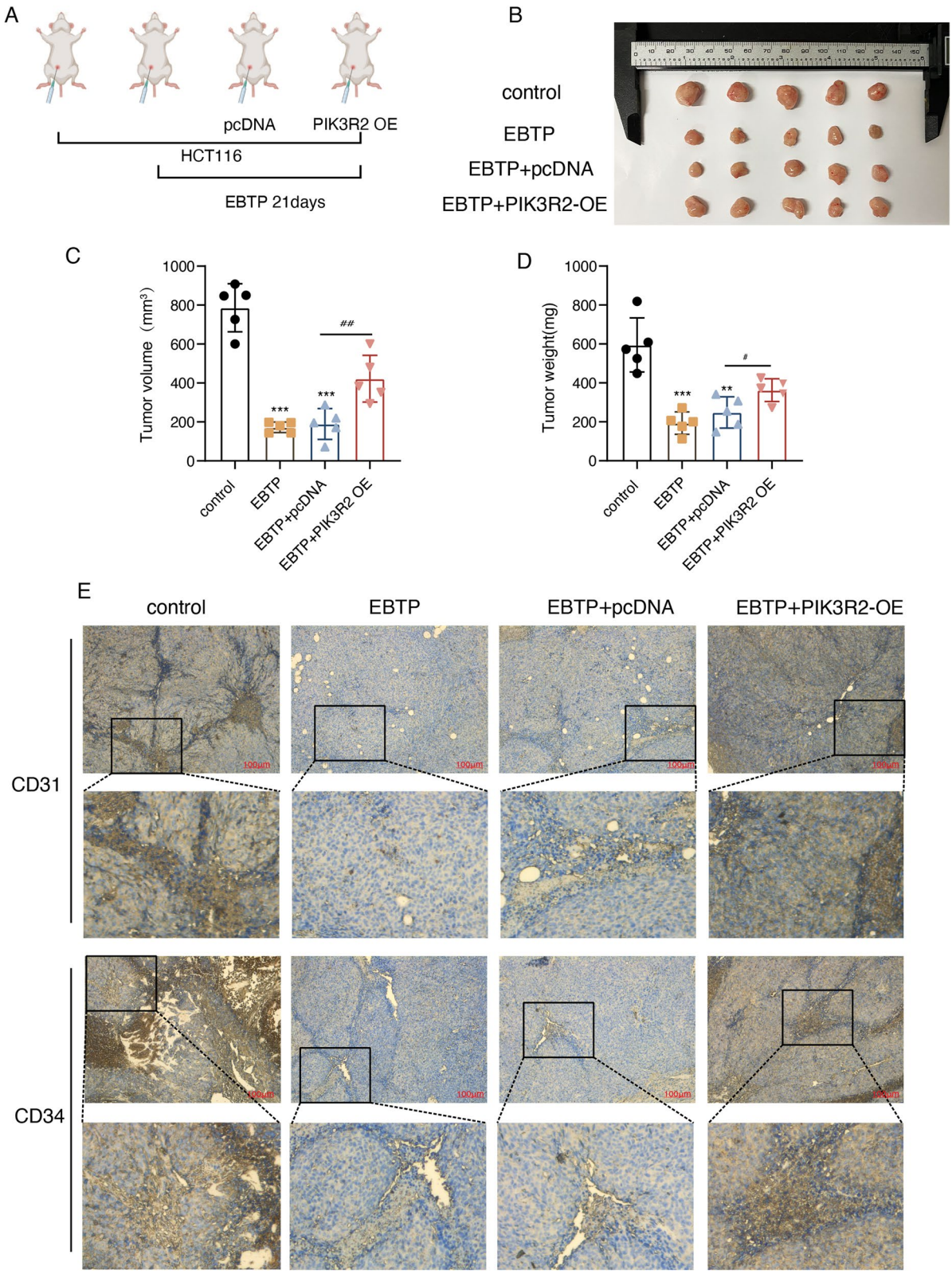

Fig. 4 (See legend on previous page.)

potential and tube-forming ability of HUVEC. VEGF pathway-related protein expression was elevated, while the opposite was restricted (Fig. 2G and H, and I). Similarly, loss-of-function and gain-of-function assays were performed in SW480 cells, showing similar results. Therefore, PIK3R2 expression promoted proliferation, migration, and angiogenesis in SW480 cells (Figure S1C-I). The experimental results indicated that PIK3R2 could exert oncogenic activity among CRC cells.

The ability of EBTP to inhibit angiogenesis in colorectal cancer depends on PIK3R2

The oncogenic activity of PIK3R in CRC cells is known. However, whether EBTP inhibition of CRC angiogenesis depends on the down-regulation of PIK3R2 expression is unclear. First, we explored the effect of EBTP on PIK3R2 expression in CRC cells based on a concentration and time gradient (Fig. 3A). EBTP suppressed the protein expression of PIK3R2 in HCT116 and SW480 cells in a concentration-dependent and time-dependent manner. EBTP also down-regulated the PIK3R2 mRNA expression in CRC cells. The PIK3R2 mRNA expression level gradually decreased by enhancing the duration or concentration of EBTP action (Fig. 3B). Next, whether CRC angiogenesis inhibition by EBTP depended on PIK3R2 was investigated. CRC cells transfected with PIK3R2 overexpression or blank vector plasmids were treated with 4 μM EBTP. EBTP significantly restricted the migratory potential and tube-forming ability of HUVECs. These results were reversed using PIK3R2 overexpression (Fig. 3C and D). Then, we examined the expression of VEGF pathway-related proteins in CRC cells with the Western Blot assay. The results depicted that EBTP down-regulated the expression of VEGF-A, VEGFR1, and VEGFR2. In contrast, PIK3R2 overexpression restored the expression of VEGF pathway-related proteins (Fig. 3E). All the above experimental results demonstrated that the inhibitory effect of EBTP on CRC angiogenesis is achieved by suppressing PIK3R2 expression.

EBTP inhibits colorectal cancer growth and angiogenesis in vivo

EBTP inhibited CRC angiogenesis in vitro by inhibiting PIK3R2 expression, which suggested whether EBTP could inhibit CRC development in vivo. We established a xenograft model in nude mice to investigate the role of EBTP in CRC. HCT116 cells were inoculated subcutaneously inside BALB/c nude mice. The experiment was divided into HCT116 alone, EBTP + HCT116, EBTP + pcDNA HCT116, and EBTP + PIK3R2 OE HCT116 groups (Fig. 4A). The results suggested that EBTP inhibited mouse tumor growth in vivo (Fig. 4B). The tumor volume and weight of mice were lower than the control group, while PIK3R2 overexpression enhanced the tumor volume and weight (Fig. 4C and D). IHC results showed that EBTP reduced the expression of CD31 and CD34, while the phenomenon was reversed by PIK3R2 overexpression (Fig. 4E). Therefore, EBTP depends on PIK3R2 to suppress CRC growth and cellular angiogenesis in vivo.

EBTP inhibits PI3K/AKT pathway phosphorylation by downregulating the expression of PIK3R2

Initially, we explored the effect of EBTP on the PI3K/AKT pathway to evaluate the downstream signaling pathway of EBTP acting on PIK3R2 since PIK3R2 is a common PI3K subunit. The results are represented in Fig. 5A. EBTP significantly inhibited the expression of total PI3K/AKT protein and its phosphorylated proteins, while PIK3R2 overexpression increased the phosphorylation level of the PI3K/AKT pathway within CRC cells (Fig. 5A). Then, the PI3K and AKT-specific activator Recilisib were used to determine whether EBTP inhibited CRC angiogenesis by suppressing PI3K/AKT phosphorylation. After describing that Recilisib effectively activates PI3K and AKT phosphorylation (Fig. 5B), the tube formation ability of HUVECs was examined. EBTP effectively inhibited HUVEC migration, while Recilisib reversed this effect (Fig. 5C). Recilisib reversed the inhibition of HUVEC migration because of EBTP in the Transwell assay (Fig. 5D). The results in Fig. 5E depict that Recilisib could restore EBTP inhibition of VEGF pathway-related protein expression. Therefore, EBTP inhibition of PIK3R2 expression in CRC cells suppressed intracellular PI3K/AKT pathway phosphorylation, inhibiting CRC angiogenesis.

EBTP indirectly regulates PIK3R2 expression via the TMPO-AS1/miR-126-3p axis and inhibits colorectal cancer angiogenesis

Many studies observed that lncRNAs are essential for different biological functions in cancer. They could act as competing endogenous RNAs (ceRNAs) to control mRNA

(See figure on next page.)

Fig. 5 EBTP inhibits PI3K/AKT pathway phosphorylation by downregulating PIK3R2 expression. **A** Western blot analysis determined the EBTP effect on the PI3K/AKT pathway proteins in CRC cells. **B** Western Blot helped assess the efficiency of PI3K/AKT-specific activator Recilisib. **C** The Tube formation experiment assessed whether Recilisib could restore the EBTP inhibitory effect on angiogenesis. **D** The Transwell experiment determined the effect of Recilisib on the migration ability of HUVEC. **E** The Western Blot experiment evaluated the Recilisib effect on the expression of VEGF pathway-related proteins. All the experiments were independently repeated thrice. *$p < 0.05$; **$p < 0.01$; ***$p < 0.001$。 #$p < 0.05$; ##$p < 0.01$; ###$p < 0.001$

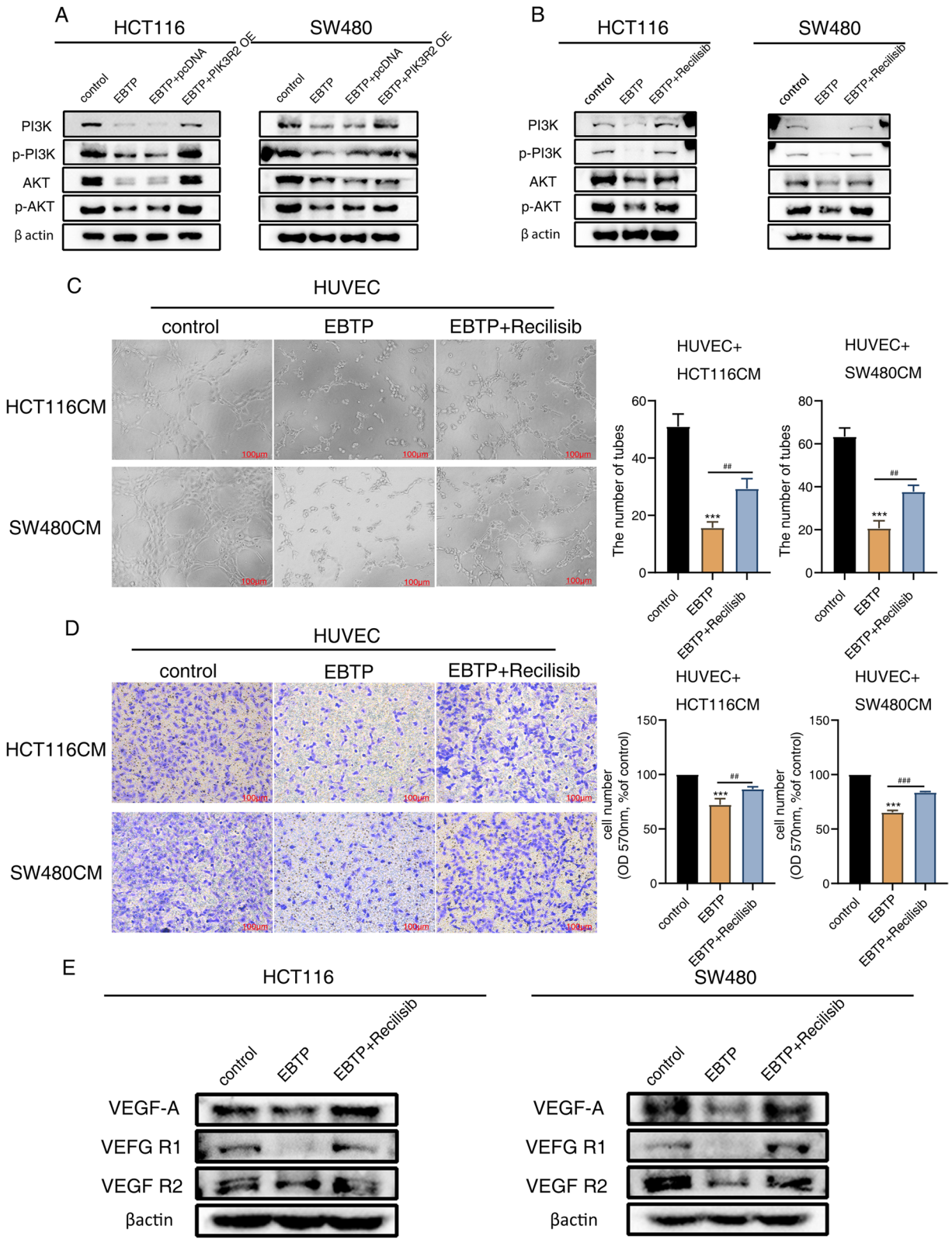

Fig. 5 (See legend on previous page.)

expression by targeting miRNAs [18, 19]. We speculated whether EBTP could indirectly regulate PIK3R2 expression and control CRC angiogenesis by mediating the expression of lncRNA or miRNA. miR-126-3p was linked with lung and hepatocellular carcinoma progression by targeting PIK3R2 [20, 21]. In contrast, lncRNA TMPO-AS1 targeted miR-126-3p to improve epithelial-mesenchymal transition in the hepatocellular carcinoma [22]. Therefore, whether the TMPO-AS1/miR-126-3p axis could regulate PIK3R2 expression and affect CRC angiogenesis was investigated. qRT-PCR results revealed that miR-126-3p expression was progressively upregulated among CRC cells, enhancing EBTP action time or concentration (Fig. 6A). In contrast, lncRNA TMPO-AS1 expression was progressively downregulated (Fig. 6B). We first predicted the respective binding sites to demonstrate the targeting between PIK3R2/TMPO-AS1 and miR-126-3p (Figure S2A). Dual luciferase reporter results suggested that the luciferase activity of the wild-type PIK3R2 reporter gene (WT PIK3R2) was significantly reduced by overexpression of miR-126-3p. However, the luciferase activity of the mutant PIK3R2 reporter gene (MUT PIK3R2) was unaffected. Similarly, miR-126-3p mimics cotransfected with WT TMPO-AS1 significantly decreased luciferase activity. Contrastingly, luciferase activity was unchanged in cells cotransfected with miR-126-3p mimics and MUT TMPO-AS1 (Fig. 6C, Figure S2B). Western Blot demonstrated that miR-126-3p inhibitor effectively upregulated PIK3R2 expression. Thus, miR-126-3p inhibitor cotransfected using sh-TMPO-AS1 restored PIK3R2 expression to its original levels (Fig. 6D). Finally, Tube formation and Transwell assays showed that miR-126-3p inhibitor significantly improved migration and tube formation in HUVECs. However, sh-TMPO-AS1 could reverse this phenomenon. Therefore, EBTP could indirectly control PIK3R2 expression via the TMPO-AS1/miR-126-3p axis, suppressing CRC angiogenesis.

Discussion

The survival rates for cancer patients have significantly improved over the past few years through preventive screening and advanced treatments. However, colorectal cancer remains the third most common malignancy globally and the leading cause of cancer-associated mortalities [23]. The pathogenesis of most patients remains unclear. However, many signaling pathways in CRC regulate biological behaviors like cell proliferation, differentiation, angiogenesis, and apoptosis [24]. In normal tissue, angiogenesis is transiently switched on. In contrast, tumor tissue continuously generates new blood vessels in response to nutrients and oxygen requirements [25]. As a cancer hallmark, angiogenesis is closely related to tumor growth, metastasis, invasion, prognosis, and recurrence [26–29]. Therefore, understanding the mechanism of CRC angiogenesis can inhibit CRC development.

Angiogenesis is essential in developing CRC, and VEGF is a classical angiogenesis pathway [30]. Our previous studies have described that EBTP could inhibit angiogenesis in hepatocellular carcinoma through the VEGF and EGFR pathways [8]. However, the exact mechanism in cancer cells remains unclear. Therefore, we first demonstrated that EBTP inhibited the proliferation, migration, and angiogenesis of CRC cells while inhibiting the VEGF pathway using various in vitro experiments (Fig. 1). Then, we used gene sequencing to obtain mRNAs with significant changes in expression in HCT116 cells with EBTP treatment and investigate the target of EBTP in CRC. We observed that EBTP had binding sites to PIK3R2 by molecular docking (Fig. 2A). Due to the high expression of PIK3R2 in CRC (Fig. 2B), PIK3R2 overexpression and PIK3R2 knockdown plasmids were constructed to determine the PIK3R2 role in CRC progression (Fig. 2C-D). The results showed that PIK3R2 overexpression effectively enhanced proliferation, migration, and angiogenesis in CRC cells. Conversely, PIK3R2 expression knockdown in CRC cells suppressed related malignant biological functions (Fig. 2E-I). Further experiments indicated that EBTP inhibited the PIK3R2 protein expression and mRNA levels in CRC cells in a time-dependent and concentration-dependent manner. Thus, PIK3R2 overexpression reversed the anti-angiogenic effect of EBTP (Fig. 3). Moreover, inhibiting angiogenesis using EBTP by controlling PIK3R2 expression was validated in vivo (Fig. 4).

(See figure on next page.)

Fig. 6 EBTP indirectly regulates PIK3R2 expression through the TMPO-AS1/miR-126-3p axis, inhibiting angiogenesis in colorectal cancer. **A** qRT-PCR helped detect the EBTP effect on miR-126-3p expression in CRC cells. **B** CRC cells treated with EBTP at different concentrations or times were subjected to qRT-PCR to determine the TMPO-AS1 expression level in the cells. **C** The Luciferase activity in HCT116 cells was detected after co-transfection of miR-126-3p mimics using WT PIK3R2 or MUT PIK3R2. After the co-transfection of miR-126-3p mimics with WT TMPO-AS1 or MUT TMPO-AS1, the Luciferase activity could be detected in HCT116 cells. **D** Western Blot helped detect whether the TMPO-AS1/miR-126-3p axis could regulate the PIK3R2 protein expression in CRC cells. **E** Transfection of miR-126-3p inhibitor or co-transfection of miR-126-3p inhibitor with sh-TMPO-AS1 helped detect the number of HUVEC tubes. **F** The Transwell experiment helped detect the effect of the TMPO-AS1/miR-126-3p axis on the migration potential of HUVECs in CRC cells. All the experiments were independently repeated thrice. *$p < 0.05$; **$p < 0.01$; ***$p < 0.001$ 。 #$p < 0.05$; ##$p < 0.01$; ###$p < 0.001$

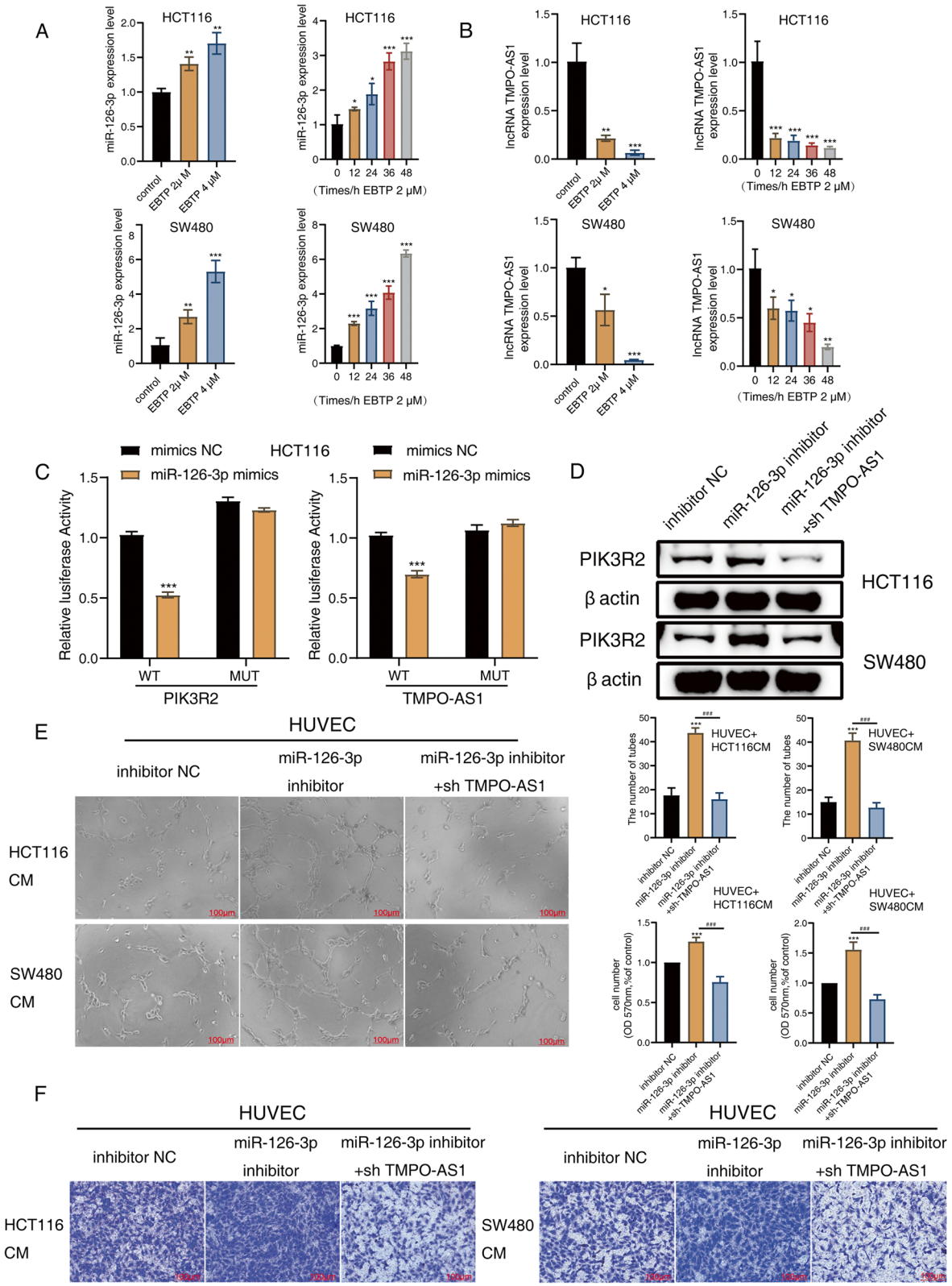

Fig. 6 (See legend on previous page.)

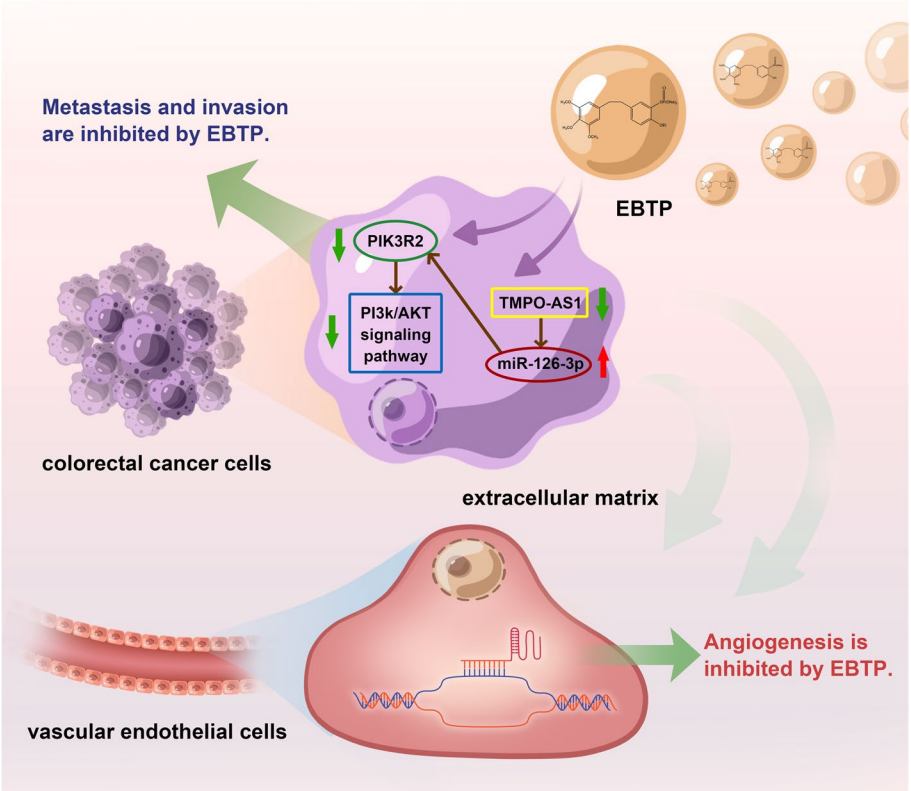

Fig. 7 Molecular mechanisms EBTP inhibits colorectal cancer metastasis, invasion, and angiogenesis

PIK3R2 is one of the common subunits of PI3K, with increasing evidence that it acts as a driver in tumor malignant progression [31, 32]. Phosphatidylinositol 3 kinases (PI3Ks) are key coordinators of signals from extracellular stimuli to the intracellular level [33]. AKT is a highly activated kinase in human cancers [34]. Abnormalities and genetic alterations across all three AKT isoforms have been identified in many cancers [35]. Our study observed that EBTP inhibited PI3K/AKT phosphorylation in CRC cells. Moreover, PI3K/AKT-specific agonists restored the tube-forming capacity in HUVECs (Fig. 5). These data suggested that EBTP inhibited PIK3R2 expression and suppressed PI3K/AKT pathway activation in CRC cells, suppressing angiogenesis. The current anti-angiogenic effect of PI3K inhibitors has enhanced the treatment outcome of cancer patients in advanced stages [36]. Therefore, further studies can explore whether EBTP could be combined with PI3K inhibitors to provide a better therapeutic index.

Long non-coding RNAs (lncRNAs) are more than 200 nucleotides long without protein-coding capacity [37]. lncRNAs have been recognized as a critical regulator involved in tumor progression [38]. microRNAs (miRNAs) are single-stranded RNA molecules of 20–23 nucleotides regulating intracellular mRNA expression by binding to 3'-untranslated regions (3'-UTRs) or amino acid coding sequences [37, 39]. We observed that miR-126-3p could target PIK3R2 to participate in cancer progression and clarify the upstream PIK3R2 mechanism [20, 21]. lncRNA TMPO-AS1 targeted miR-126-3p to improve epithelial-mesenchymal transition in hepatocellular carcinoma [22]. In addition, miR-126 is highly expressed in vascular endothelial cells and is a significant regulator of vascular integrity and physiological angiogenesis [40, 41]. miR-126 downregulation is observed in different malignancies [42]. Our results revealed that EBTP could inhibit TMPO-AS1 expression and promote miR-126-3p expression. The simultaneous dual-luciferase assay confirmed the binding of PIK3R2 and miR-126-3p and the targeting of miR-126-3p and TMPO-AS1. Functional assay results showed that the TMPO-AS1/miR-126-3p axis could control PIK3R2 expression and CRC angiogenesis (Fig. 6).

Therefore, EBTP could indirectly inhibit PIK3R2 expression through the TMPO-AS1/miR-126-3p axis. This inhibits PI3K/AKT phosphorylation in CRC cells and suppresses CRC angiogenesis. Our study clarified the specific mechanism of EBTP inhibition of CRC angiogenesis (Fig. 7). Moreover, the newly discovered TMPO-AS1/miR-126-3p/PIK3R2/PI3K/AKT axis provided insights into angiogenesis and a novel strategy for treating CRC.

Abbreviations

CRC	Colorectal cancer
EBTP	Ethoxy-erianin phosphate
TMPO-AS1	TMPO antisense RNA 1
PIK3R2	Phosphoinositide-3-kinase regulatory subunit 2
PI3K	Phosphatidylinositol 3-kinase
P-PI3K	Phospho-phosphatidylinositol 3-kinase
AKT	AKT serine/threonine kinase 1
P-AKT	Phospho-AKT serine/threonine kinase 1
VEGF	Vascular endothelial growth factor
EGFR	Epidermal growth factor receptor
lncRNA	Long non-coding RNA
HUVEC	Human umbilical vein endothelial cells
PBS	Phosphate-buffered saline
RT-qPCR	Reverse transcription-quantitative polymerase chain reaction
SDS	Sodium dodecyl sulfate
SDS-PAGE	SDS-polyacrylamide
VEGF-A	Vascular endothelial growth factor-A
VEGFR1	Vascular endothelial growth factor receptor 1
VEGFR2	Vascular endothelial growth factor receptor 2
SP	Standard Precision
GAPDH	Glyceraldehyde-3-phosphate dehydrogenase
U6	U6 small nuclear RNA
IACUC	Institutional Animal Care and Use Committee
IHC	Immunohistochemistry
ceRNAs	Competing endogenous RNAs

Supplementary Information

The online version contains supplementary material available at https://doi.org/10.1186/s12885-024-12893-4.

Supplementary Material 1.

Supplementary Material 2.

Supplementary Material 3.

Acknowledgements
Not applicable.

Authors' contributions
Study concept and design:ZWM, SC and CYO; Performed the experiment: LSQ, LYX and ZYQ; Data analysis and interpretation: LX, WFH and LJW; Manuscript writing and review: TF. All authors have read and approved the manuscript in its current state.

Funding
This study was supported by grants from the Shanghai Minhang District high level specialist doctor training program (Grant Nos. 2020MZYS15); Shanghai Minhang District large-scale discipline construction project (Grant Nos. 2017MWDXK03); Shanghai Minhang Science and Technology Commission (CN) (Grant Nos. 2023MHZ072); Fundamental Medical Project of Minhang Hospital of Fudan University Project Foundation (Grant Nos. 2022MHBJ03);

Availability of data and materials
PIK3R2 expression were gathered from openly available databases including the HPA website (https://www.proteinatlas.org/) and the GEPIA website (http://gepia.cancer-pku.cn/). Other data that support the findings of this study are available on request from the corresponding author.

Declarations

Ethics approval and consent to participate
All animal studies were performed with approval from the Institutional Animal Care and Use Committee of Fudan University. The study is accordance with ARRIVE guidelines. Clinical trial number: not applicable.

Consent for publication
Not applicable.

Competing interests
The authors declare no competing interests.

Author details
[1]Department of Gastrointestinal Surgery, Minhang Hospital, Fudan University, Shanghai, China. [2]Key Laboratory of Whole-period Monitoring and Precise Intervention of Digestive Cancer (SMHC), Minhang Hospital & AHS, Fudan University, Shanghai, China. [3]Shanghai Frontiers Science Center of Optogenetic Techniques for Cell Metabolism, Shanghai Key Laboratory of New Drug Design, School of Pharmacy, East China University of Science and Technology, Shanghai, China. [4]Department of Endoscope Center, Minhang Hospital, Fudan University, Shanghai, China. [5]School of Chemical and Environmental Engineering, Shanghai Institute of Technology, Shanghai, China. [6]Zhejiang Guangsha Vocational and Technical University of Construction, Jinhua, China.

Received: 3 December 2023 Accepted: 3 September 2024
Published online: 14 October 2024

References

1. Siegel RL, Miller KD, Jemal A. Cancer statistics, 2018. CA Cancer J Clin. 2018;68(1):7–30.
2. Barzi A, Lenz HJ, Quinn DI, Sadeghi S. Comparative effectiveness of screening strategies for colorectal cancer. Cancer. 2017;123(9):1516–27.
3. Zhao J, Ou B, Han D, Wang P, Zong Y, Zhu C, Liu D, Zheng M, Sun J, Feng H, et al. Tumor-derived CXCL5 promotes human colorectal cancer metastasis through activation of the ERK/Elk-1/Snail and AKT/GSK3β/β-catenin pathways. Mol Cancer. 2017;16(1):70.
4. Zhu CC, Chen C, Xu ZQ, Zhao JK, Ou BC, Sun J, Zheng MH, Zong YP, Lu AG. CCR6 promotes tumor angiogenesis via the AKT/NF-κB/VEGF pathway in colorectal cancer. Biochim Biophys Acta Mol Basis Dis. 2018;1864(2):387–97.
5. Battaglin F, Puccini A, Intini R, Schirripa M, Ferro A, Bergamo F, Lonardi S, Zagonel V, Lenz HJ, Loupakis F. The role of tumor angiogenesis as a therapeutic target in colorectal cancer. Expert Rev Anticancer Ther. 2018;18(3):251–66.
6. Chen P, Wu Q, Feng J, Yan L, Sun Y, Liu S, Xiang Y, Zhang M, Pan T, Chen X, et al. Erianin, a novel dibenzyl compound in Dendrobium extract, inhibits lung cancer cell growth and migration via calcium/calmodulin-dependent ferroptosis. Signal Transduct Target Ther. 2020;5(1):51.
7. Yuan W, Su C, Yang X, Li Y, Cao Y, Liang X, Liu J. Biological and anti-vascular activity evaluation of ethoxy-erianin phosphate as a vascular disrupting agent. J Cell Biochem. 2019;120(10):16978–89.
8. Chen J, Liu J, Xu B, Cao Y, Liang X, Wu F, Shen X, Ma X, Liu J. Ethoxy-erianin phosphate and afatinib synergistically inhibit liver tumor growth and angiogenesis via regulating VEGF and EGFR signaling pathways. Toxicol Appl Pharmacol. 2022;438:115911.
9. Herrero-Gonzalez S, Di Cristofano A. New routes to old places: PIK3R1 and PIK3R2 join PIK3CA and PTEN as endometrial cancer genes. Cancer Discov. 2011;1(2):106–7.
10. Hirsch E, Ciraolo E, Franco I, Ghigo A, Martini M. PI3K in cancer-stroma interactions: bad in seed and ugly in soil. Oncogene. 2014;33(24):3083–90.
11. Fruman DA, Chiu H, Hopkins BD, Bagrodia S, Cantley LC, Abraham RT. The PI3K pathway in Human Disease. Cell. 2017;170(4):605–35.
12. Wang Y, Peng J, Bai S, Yu H, He H, Fan C, Hao Y, Guan Y. A PIK3R2 mutation in familial temporal lobe Epilepsy as a possible pathogenic variant. Front Genet. 2021;12:596709.
13. Fu R, Tong JS. miR-126 reduces trastuzumab resistance by targeting PIK3R2 and regulating AKT/mTOR pathway in breast cancer cells. J Cell Mol Med. 2020;24(13):7600–8.
14. Xu HF, Huang TJ, Yang Q, Xu L, Lin F, Lang YH, Hu H, Peng LX, Meng DF, Xie YJ, et al. Candidate tumor suppressor gene IRF6 is involved in human breast cancer pathogenesis via modulating PI3K-regulatory subunit PIK3R2 expression. Cancer Manag Res. 2019;11:5557–72.
15. Zhou J, Xu N, Liu B, Wang C, He Z, Lenahan C, Tang W, Zeng H, Guo H. lncRNA XLOC013218 promotes cell proliferation and TMZ resistance by targeting the PIK3R2-mediated PI3K/AKT pathway in glioma. Cancer Sci. 2022;113(8):2681–92.

16. Song L, Xie X, Yu S, Peng F, Peng L. MicroRNA–126 inhibits proliferation and metastasis by targeting pik3r2 in prostate cancer. Mol Med Rep. 2016;13(2):1204–10.
17. Yan L, Zhang Z, Liu Y, Ren S, Zhu Z, Wei L, Feng J, Duan T, Sun X, Xie T, et al. Anticancer activity of erianin: Cancer-Specific Target Prediction based on Network Pharmacology. Front Mol Biosci. 2022;9:862932.
18. Peng WX, Koirala P, Mo YY. LncRNA-mediated regulation of cell signaling in cancer. Oncogene. 2017;36(41):5661–7.
19. Smolarz B, Zadrożna-Nowak A, Romanowicz H. The role of lncRNA in the development of tumors, including breast cancer. Int J Mol Sci. 2021;22(16):8427.
20. Di Paolo D, Pontis F, Moro M, Centonze G, Bertolini G, Milione M, Mensah M, Segale M, Petraroia I, Borzi C, et al. Cotargeting of mir-126-3p and mir-221-3p inhibits PIK3R2 and PTEN, reducing lung cancer growth and metastasis by blocking AKT and CXCR4 signalling. Mol Oncol. 2021;15(11):2969–88.
21. Du C, Lv Z, Cao L, Ding C, Gyabaah OA, Xie H, Zhou L, Wu J, Zheng S. MiR-126-3p suppresses tumor metastasis and angiogenesis of hepatocellular carcinoma by targeting LRP6 and PIK3R2. J Transl Med. 2014;12:259.
22. Huang W, Chen Q, Dai J, Zhang Y, Yi Y, Wei X. Long noncoding TMPO antisense RNA 1 promotes hepatocellular carcinoma proliferation and epithelial-mesenchymal transition by targeting the microRNA-126-3p/LRP6/β-catenin axis. Ann Transl Med. 2021;9(22):1679.
23. Wong A, Ma BB. Personalizing therapy for colorectal cancer. Clin Gastroenterol Hepatol. 2014;12(1):139–44.
24. Fearon ER. Molecular genetics of colorectal cancer. Annu Rev Pathol. 2011;6:479–507.
25. Hanahan D, Weinberg RA. Hallmarks of cancer: the next generation. Cell. 2011;144(5):646–74.
26. He L, Zhu W, Chen Q, Yuan Y, Wang Y, Wang J, Wu X. Ovarian cancer cell-secreted exosomal miR-205 promotes metastasis by inducing angiogenesis. Theranostics. 2019;9(26):8206–20.
27. Zhang L, Kundu S, Feenstra T, Li X, Jin C, Laaniste L, El Hassan TE, Ohlin KE, Yu D, Olofsson T, et al. Pleiotrophin promotes vascular abnormalization in gliomas and correlates with poor survival in patients with astrocytomas. Sci Signal. 2015;8(406):ra125.
28. Zhu P, Wu Y, Yang A, Fu X, Mao M, Liu Z. Catalpol suppressed proliferation, growth and invasion of CT26 colon cancer by inhibiting inflammation and tumor angiogenesis. Biomed Pharmacother. 2017;95:68–76.
29. Cao J, Liu X, Yang Y, Wei B, Li Q, Mao G, He Y, Li Y, Zheng L, Zhang Q, et al. Decylubiquinone suppresses breast cancer growth and metastasis by inhibiting angiogenesis via the ROS/p53/ BAI1 signaling pathway. Angiogenesis. 2020;23(3):325–38.
30. Itatani Y, Kawada K, Yamamoto T, Sakai Y. Resistance to anti-angiogenic therapy in cancer-alterations to anti-VEGF pathway. Int J Mol Sci. 2018;19(4):1232.
31. Cortés I, Sánchez-Ruíz J, Zuluaga S, Calvanese V, Marqués M, Hernández C, Rivera T, Kremer L, González-García A. Carrera AC: p85β phosphoinositide 3-kinase subunit regulates tumor progression. Proc Natl Acad Sci U S A. 2012;109(28):11318–23.
32. Vallejo-Díaz J, Chagoyen M, Olazabal-Morán M, González-García A, Carrera AC. The opposing roles of PIK3R1/p85α and PIK3R2/p85β in Cancer. Trends Cancer. 2019;5(4):233–44.
33. Noorolyai S, Shajari N, Baghbani E, Sadreddini S, Baradaran B. The relation between PI3K/AKT signalling pathway and cancer. Gene. 2019;698:120–8.
34. Vasudevan KM, Barbie DA, Davies MA, Rabinovsky R, McNear CJ, Kim JJ, Hennessy BT, Tseng H, Pochanard P, Kim SY, et al. AKT-independent signaling downstream of oncogenic PIK3CA mutations in human cancer. Cancer Cell. 2009;16(1):21–32.
35. Zinda MJ, Johnson MA, Paul JD, Horn C, Konicek BW, Lu ZH, Sandusky G, Thomas JE, Neubauer BL, Lai MT, et al. AKT-1, -2, and – 3 are expressed in both normal and tumor tissues of the lung, breast, prostate, and colon. Clin Cancer Res. 2001;7(8):2475–9.
36. Suvarna V, Murahari M, Khan T, Chaubey P, Sangave P. Phytochemicals and PI3K inhibitors in Cancer-An Insight. Front Pharmacol. 2017;8:916.
37. Quan M, Chen J, Zhang D. Exploring the secrets of long noncoding RNAs. Int J Mol Sci. 2015;16(3):5467–96.
38. Cheng J, Chen J, Zhang X, Mei H, Wang F, Cai Z. Overexpression of CRNDE promotes the progression of bladder cancer. Biomed Pharmacother. 2018;99:638–44.
39. Li Y, Liang Y, Sang Y, Song X, Zhang H, Liu Y, Jiang L, Yang Q. MiR-770 suppresses the chemo-resistance and metastasis of triple negative breast cancer via direct targeting of STMN1. Cell Death Dis. 2018;9(1):14.
40. Wang Y, Sun J, Kahaleh B. Epigenetic down-regulation of microRNA-126 in scleroderma endothelial cells is associated with impaired responses to VEGF and defective angiogenesis. J Cell Mol Med. 2021;25(14):7078–88.
41. Zhou Q, Anderson C, Hanus J, Zhao F, Ma J, Yoshimura A, Wang S. Strand and cell type-specific function of microRNA-126 in Angiogenesis. Mol Ther. 2016;24(10):1823–35.
42. Ebrahimi F, Gopalan V, Smith RA, Lam AK. miR-126 in human cancers: clinical roles and current perspectives. Exp Mol Pathol. 2014;96(1):98–107.

Publisher's note